# Open Archive TOULOUSE Archive Ouverte (OATAO)

OATAO is an open access repository that collects the work of Toulouse researchers and makes it freely available over the web where possible.

# High power density aqueous hybrid supercapacitor combining activated carbon and highly conductive spinel cobalt oxide

G. Godillot [a], P.-L. Taberna [b, c], B. Daffos [b, c], P. Simon [b, c], C. Delmas [a],
L. Guerlou-Demourgues [a, c, z]

[a] CNRS, Univ. Bordeaux, Bordeaux INP, ICMCB UPR 9048, F-33600, Pessac, France
[b] CIRIMAT UMR 5085, Université de Toulouse, 118 Route de Narbonne, F-31062, Toulouse, France
[c] RS2E, Réseau Français sur le Stockage Electrochimique de l'Energie, FR CNRS 3459, France

## HIGHLIGHTS

- Original conductive nano cobalt oxide is used in hybrid C/Co supercap.
- The positive/negative ratio was optimized.
- Best performances for a positive/negative weight ratio of 1.25.
- This system is among the best ones of its category (61.6 F g$^{-1}$).
- The system exhibits excellent electrochemical ageing over 3000 cycles.

## ABSTRACT

The remarkable electrochemical behavior of complete activated carbon/cobalt oxide cells is reported in the present work. Among the various weight ratios between the positive and negative electrodes evaluated, the best features are obtained with an overcapacitive cobalt oxide electrode. The energy densities obtained by this system (20 Wh kg$^{-1}$ for a power density of 209 W kg$^{-1}$) are twice higher than those measured for a activated carbon/activated carbon symmetric cell, in the same operating conditions. With discharge capacities around 62 F g$^{-1}$, this system is among the best ones reported in the literature for this category.

## 1. Introduction

Numerous investigations on supercapacitors are focusing on increasing energy densities, in particular with the development of hybrid "metal oxide/activated carbon" supercapacitors [1]. We recently reported the potentialities of original nanometric conductive cobalt oxides, with spinel structure, as positive electrode of supercapacitor in alkaline medium [2,3]. These phases, which were synthesized by oxidizing precipitation of cobalt nitrate in a basic medium (T < 90 °C), exhibit a modified spinel - $Co_3O_4$ type structure, with protons, lithium and cobalt vacancies, as well as $Co^{4+}$ ions in the octahedral trivalent cobalt network [4–6]. Such octahedral tetravalent cobalt ions entail electronic delocalization and very good electronic conductivity properties ($5 \times 10^{-4}$ S cm$^{-1}$, against $10^{-6}$ S cm$^{-1}$ for ideal $Co_3O_4$), which can still be improved by a controlled thermal treatment at a moderate temperature (200 °C), while keeping particle size and specific surface area (200 m$^2$ g$^{-1}$) suitable for electrochemical cycling [5,6].

These materials, mixed with additional organic binder and carbon black, were then conditioned as autosupported thin films, which were pasted on current collector, and then characterized by various electrochemical techniques (chronoamperometry, potentiometry, impedance spectrometry, cyclic voltametry), in a classical three-electrode cell configuration, filled with a 5M-KOH electrolyte [3]. The electrochemical properties of the materials were also

evaluated in a cavity microelectrode. The overall results, based on combined electrochemical, X ray diffraction and microscopy studies of the electrodes, tend to prove that redox reactions take place during cycling at the very surface of the materials (on a depth in the range of 10 Å). With capacity values reaching 70 mAh g$^{-1}$ at 5 mV s$^{-1}$, our cobalt oxides compete favorably with other metal oxides reported in the literature as electrode materials for supercapacitors. Only a very small amount of added carbon black is necessary to get optimized capacities in the case of our materials (5% carbon added only against often more than 20% for the major part of studies reported in the literature for this kind of materials).

The work reported in this paper aims at evaluating the performances of complete hybrid cells assembling an optimized positive electrode based on our conductive spinel cobalt oxide, with a negative microporous active carbon electrode, in alkaline medium (5M-KOH). The combination of a positive electrode based on our cobalt oxides (electrochemically active between 0.1 and 0.7 V vs SHE) and of an activated carbon electrode, electrochemically active in the whole stability domain of water, should lead to a system exhibiting an electrochemical activity window higher than that reached for the cobalt material alone. Moreover, the activated carbon (AC)/nano-cobalt oxide hybrid system is expected to benefit from the different natures and advantages of its two electrodes: EDLC-type for the former one, which leads to a good behavior at high power and to an excellent cycle ability, and redox-type electrode for the latter one, which leads to a high capacity.

After a preliminary electrochemical evaluation of the two electrode materials in KOH electrolyte, the two electrodes will be balanced in order to determine the optimized configuration. Special attention will be paid to the electrochemical ageing.

## 2. Experimental

### 2.1. Material preparation

As described in detail in a previous paper [4], nano-spinel type cobalt oxide was prepared by precipitation at 90 °C of a cobalt salt in a 8M-KOH + 0.5M-NaOH + 0.5M-LiOH alkaline solution. Cobalt nitrate hexahydrate (Fluka) was dissolved into distilled water, mixed with hydrogen peroxide (Fluka) (with a $Co(NO_3)_2$:$H_2O_2$ molar ratio of 3:2), and then added drop-wise to the ternary alkaline solution to induce precipitation of the nanometric cobalt oxide. The suspension obtained was allowed to ripen for 4 h at 90 °C. Afterward, the precipitate was centrifuged and washed with distilled water until neutrality, and then dried at 60 °C for 24 h. As previously reported, X ray diffraction confirms the spinel structure of this material, with the presence of structural defects which are responsible for the good electronic conductivity observed ($5 \times 10^{-4}$ S cm$^{-1}$). The specific area of this material is close to 200 m$^2$ g$^{-1}$. The nanostructure of the material is illustrated in Supplementary Fig. 1. The material is constituted of polydisperse agglomerates of nano-crystallites, with size of 5−10 Å.

Since cobalt oxide (positive electrode) was the main object of the present study, activated carbon (AC) for the negative electrode of the supercapacitor was not really optimized. Commercial activated carbon YP-17, provided by Kuraray (Japan), was selected for its good electronic properties and its high specific area (1600 m$^2$/g).

### 2.2. Electrode preparation

As far as spinel nano cobalt oxide is concerned, a proper amount of powdered material, 5% in mass PTFE (Dupont de Nemours), and 5% of carbon black (conductive additive made of acetylene, 100% compressed, Alfa Aesar) were mixed with ethanol. The mixture was set as an autosupported film, in which a 11 mm-diameter disc was cut and then pressed on nickel foam (current collector) at 100 MPa. The electrode was finally dried at 60 °C for 12 h. Electrodes based on activated carbon are prepared according to the same procedure, but without carbon black added.

### 2.3. Electrochemical characterization

The preliminary study reported in section 3.1 was performed with a three-electrode cell (classical corrosion cell from Radiometer Analytical, France), filled with a 5M-KOH electrolyte. The preparation of the working electrodes (cobalt oxide or activated carbon) is detailed just above. Platinum was used as counter electrode and HgO/Hg as reference electrode. Cyclic voltammetry was completed using a VMP3 potentiostat (Biologic).

The other electrochemical measurements were performed in a three-electrode Swagelok cell, because of its more optimized geometry. AgO/Ag was used as reference electrode. It should be noticed that the cells were not sealed, to avoid any overpressure hazard due to electrolyte oxidation.

## 3. Results and discussion

### 3.1. Preliminary study of the potential windows for activated carbon (negative electrode) and spinel cobalt oxide (positive electrode) in 5 M − KOH electrolyte

The potential window for the cobalt oxide was already discussed in details in a previous paper [3]. Voltammograms registered at 5 mV s$^{-1}$ between a minimum potential of −0.2 V and increasing maximum potentials (E$_{max}$) up to 0.80 V are shown in Fig. 1a. As can be deduced from the integration of the cathodic branches, the cathodic capacity increases with E$_{max}$ value. The coulombic efficiency, which maintains above 97% for E$_{max}$ < 0.70 V, strongly decreases for higher potential values, due to the oxidation of water based electrolyte. Between −0.2 V and 0.72 V, which is the limit value beyond which the coulombic efficiency drops, the capacity obtained for the material is 73 mAh g$^{-1}$. Note that the open circuit potentials of both cobalt and carbon electrodes are close to 0 V vs NHE.

In the case of the activated carbon, the voltammograms were collected between a maximum potential of 0.3 V and minimum potentials (E$_{min}$) decreasing from −0.3 V down to −1.1 V, as shown in Fig. 1b. The oxidation current observed above 0.3 V (vs NHE) for AC is known to be mainly due to carbon oxidation [7−9] leading to CO evolution. At the lowest potentials, below −1.0 V, the potential window of AC is limited by water reduction. Between −1.0 V and 0.3 V, the voltammogramm exhibits a near-rectangular shape, with close absolute values of anodic and cathodic currents, which is characteristic of a pure capacitive behavior (double layer capacity), reversible in this potential range [10]. The anodic capacity is around 54 mAh g$^{-1}$. This is the interesting parameter, from the application point of view, since activated carbon is intended to be used at the negative electrode of the target hybrid supercapacitor i.e. it will work in oxidation during the discharge of the supercapacitor. It should be noticed that the voltammetry curves exhibit an increase of the anodic current when the electrochemical window is enlarged towards the lowest potentials (for Emin ≤ −0.9 V), while the cathodic current remains quite stable. As shown by Jurewicz et al., polarizing the activated carbon electrode below the thermodynamic stability potential (−0.87 V in 5M-KOH) leads to produce hydrogen, which is not directly released, but adsorbed in the carbon micropores [11], and then reversibly oxidized during the anodic step. Such a process causes the observed increase of the anodic current. In addition, the lower the polarizing potential, the higher the produced hydrogen amount, and the higher the anodic
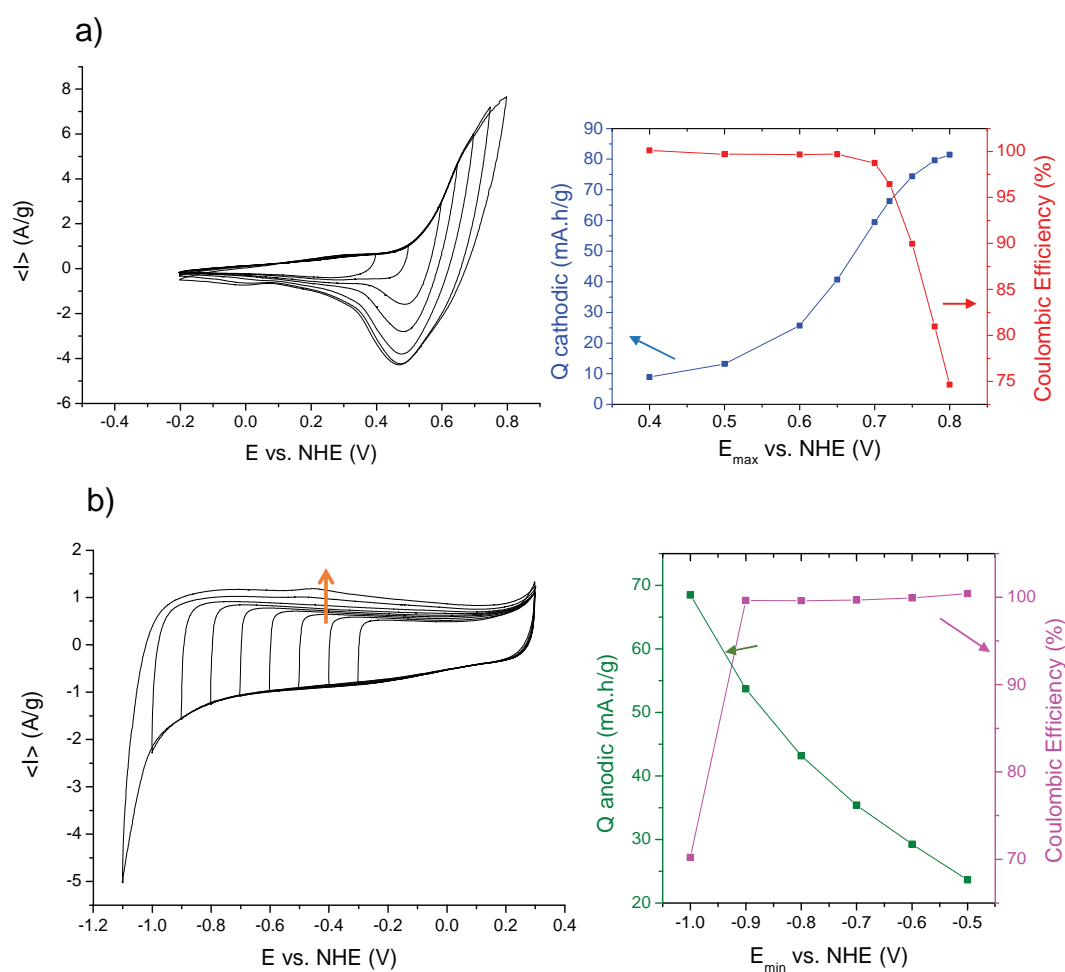
**Fig. 1.** Cyclic voltammetry curves, at 5 mV s$^{-1}$ in 5M-KOH, registered for: (a) an electrode based on our conductive spinel cobalt oxide, for potential varying between −0.2 V and maximum values ranging from 0.4 to 0.8 V vs. NHE. The variations of corresponding cathodic capacity and coulombic efficiency are also presented. (b) An activated carbon based electrode, for potential varying between 0.3 V and minimum values ranging from −0.3 V to −1.1 V. The variations of anodic capacity and coulombic efficiency extracted from galvanostatic cycling at 0.1 A g$^{-1}$ are also presented.

current that results from hydrogen electro-oxidation. The insert in Fig. 1b presents the evolution of anodic capacity (green curve) and coulombic efficiency (magenta curve) deduced from galvanostatic cycling at 0.1 A g$^{-1}$ (not reported here). For minimum potentials down to −0.9 V (included), the coulombic efficiency is close to 100%, in good accordance with the reversible capacitive behavior of activated carbon, but it drops to 70% for lower potentials, due to water reduction. In conclusion, the optimized potential window of activated carbon is between −0.9 V and 0.3 V, and the anodic capacity in this window is 54 mAh g$^{-1}$. Overall, it is here that comes out the interest of an hybrid supercapacitor. According to aforementioned results, it is expected that coupling to different kind of electrode lead to maximize the cell voltage: 1.6 V for a C-Co$_3$O$_4$ cell and only 1.2 V for a carbon-carbon cell. In other word, an increase of almost twice the maximal specific energy is expected in such hybrid cell. Nevertheless, the challenge is to find out the proper electrode balance to take advantage of this system.

### 3.2. Balance of the electrodes in the hybrid supercapacitor: effect of the electrodes mass ratio

Balancing the electrodes consists in adjusting the weights of positive and negative electrodes to obtain, for the complete cell, the highest capacity in discharge. Keeping in mind that the total capacity of the cell is monitored by the electrode with the lowest capacity, in the case of symmetric cells, the most optimized configuration is theoretically the one involving the same capacity for both electrodes. For hybrid or hybrid cells, the behavior is quite different, due to the fact that the charge storage mechanism may be different. In the case of our AC/nano-Co$_3$O$_4$ system, the electrodes are indeed very different in their electrochemical signature (faradic type storage for cobalt oxide against capacitive behavior for AC), so that it is necessary to investigate various amount ratios between the two electrodes, to determine the optimal configuration. The theoretical charge balance of the two electrodes corresponds to a ratio R = m+/m− = Q−/Q+, where m+ and m- correspond to the active material weights and Q+ and Q− to the theoretical capacities expected for the two materials (73 mAh g$^{-1}$ for cobalt oxide and 54 mAh g$^{-1}$ for AC), which leads to a value of 0.74 for R. A first study of a balanced cell is first performed in order to investigate the potential window, and other ratios such as 0.5, 1.00 and 1.25 are also studied.

### 3.2.1. Preliminary study of the voltage window limits

The voltage window limits were evaluated by cyclic voltammetry in a three-electrode cell at 5 mV s$^{-1}$. Only the results obtained for the charge balanced hybrid supercapacitor (R = 0.74) are presented here, but they are quite similar for the other investigated

ratios. The curves obtained for a voltage varying from a minimum value ($V_{min}$) of 0.5 V to maximum values ($V_{max}$) in the 1.1–1.6 V range, are displayed in Fig. 2. The minimum potential was fixed at 0.5 V because there is no significant signal corresponding to charge storage below 0.5 V.

Wide cathodic peaks are observed, with an intensity and a voltage increasing with $V_{max}$ (from 0.80 V for $V_{max}$ = 1.1 V up to 1.33 V for $V_{max}$ = 1.7 V). On account of its position, such peak can be assigned to the reduction of cobalt oxide. The higher the voltage value, the more cobalt oxide will be oxidized, the higher the intensity of the resulting reduction peak. As already observed during the cycling of the cobalt oxide electrode alone (Fig. 1a), the associated oxidation peak is probably partially hidden by the electrolyte oxidation. The second current peak observed at low potential (0.6 V) while discharging on the voltammogram registered for $V_{max}$ = 1.7 V can be attributed to the oxidation/release of a noticeable amount of hydrogen that is adsorbed in the micropores of AC after reduction of the electrolyte during the previous charge. Such behavior is responsible for the fact that the coulombic efficiency, as shown in the insert of Fig. 2, becomes slightly higher than 100%, for $V_{max} \leq 1.3$ V. On the other hand, the coulombic efficiency drops from values higher than 99% down to 96% for $V_{max}$ = 1.7 V. This confirms an important contribution of water electrolysis at this voltage. It appears therefore as reasonable to limit the voltage of the charge balanced hybrid supercapacitor to 1,60 V, in good agreement with the preliminary study of cobalt oxide and AC electrodes (Fig. 1). It should be noticed that the capacity obtained in discharge ($Q_{tot}$) between 0.5 and 1.6 V is 14.3 mAh g$^{-1}$ of active materials (AC + cobalt oxide), which is very close to the value calculated on the basis of the capacities of the two electrodes (15.5 mAh g$^{-1}$), according to the following formula: $\frac{1}{m_{tot} \times Q_{tot}} = \frac{1}{m_+ \times Q_+} + \frac{1}{m_- \times Q_-}$.

### 3.2.2. Influence of the electrodes mass ratio at low rate

In order to optimize the performances of our hybrid AC/nano-$Co_3O_4$ supercapacitor, it is necessary to test different electrodes mass ratio, other than that corresponding to a perfect balance of
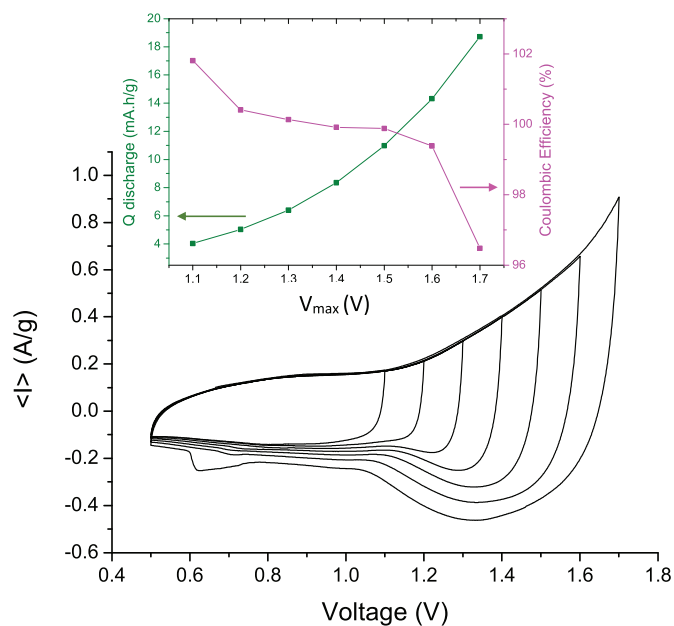


**Fig. 2.** Study of the voltage window of an AC/nano-$Co_3O_4$ charge balanced hybrid supercapacitor in a three-electrode Swagelock cell in 5M-KOH. Cyclic voltammetry curves are registered between 0.5 V and maximum voltage values ranging from 1.1 to 1.7 V. The variations of discharge capacity and coulombic efficiency are presented in insert.

positive and negative charges (R = 0.74). When the electrochemical characterization is indeed performed on one electrode, the electrode potential is perfectly controlled, whereas the potentials of the two electrodes can vary independently in a complete cell. The optimized electrodes mass ratio can therefore be different from that expected on the basis of preliminary characterizations. Demarconnay et al. have shown that the performances of an AC/$MnO_2$ supercapacitor in neutral medium are higher when the positive electrode is overcapacitive, with an optimized R ratio equal to 2.5, against 2.00 in a charge balance configuration [12]. In our case, such an effect is expected as a result of the non capacitive behavior of cobalt oxide on one hand, and of the weak overlap between the voltammograms of AC and cobalt oxide. The behaviors of the following various configurations were therefore systematically compared: one with a charge excess of activated carbon at the negative electrode (R = 0.5), two other ones with an overcapacitive cobalt oxide positive electrode (R = 1.00 and R = 1.25), and the balanced configuration (R = 0.74). In the former case it is expected that the voltage profile will be controlled by the cobalt oxide based electrode, in the latter case by the carbon electrode.

The voltammograms registered for the four configurations at 5 mV s$^{-1}$ in 5M-KOH in three-electrodes Swagelock cells, are presented in Fig. 3a. When the weight of cobalt electrode increases, i.e. for increasing R values, according to the general tendency, the voltammograms tend to be enlarged at low voltage (from 0.5 to 1.2 V), and to shrink in the 1.5–1.6 V range (cobalt oxidation and reduction peaks), except for R = 0.50 (1.1–1.5 V). These two tendencies suggest an increasing contribution of AC with R, since the electrochemical response of the system is governed by carbon at lower voltage (0.5–1.1 V) and by cobalt oxide at higher voltage. For R > 0.74, the AC electrode becomes limiting in terms of charges and prevents cobalt oxide to be oxidized/reduced as much as allowed by the accessible charge amount.

Galvanostatic cycling of the four cells, in three electrode configuration, has been performed, in order to follow the evolution of the absolute potentials of both electrodes. The results, corresponding to cycling at 0.2 A g$^{-1}$ in 5M-KOH between 0.5 and 1.6 V, are gathered in Fig. 3b. It appears clearly that, in the case of the balanced cell (R = 0.74), the windows in which the potentials of the positive and negative electrodes are placed, 0.68 and 0.43 V respectively, are roughly the same. But if a charge excess is introduced within one electrode, its potential window tends to strongly increase at the expense of that of the opposite electrode. This confirms the hypothesis of the growing participation of AC when R increases, and conversely for cobalt oxide. For R = 0.50, the contribution of AC is close to zero since the associated potential window stretches over 0.02 V. Nevertheless, for R = 1.00 and R = 1.25, the potential of the cobalt oxide electrode is fairly high (from 0.16 to 0.50 V) and is displacing in a significant potential window (0.33 and 0.22 V respectively), which should lead to reasonable capacities. It should be noticed that, in the case of R = 0.5, the potential of the AC electrode remains constant at −1.2 V, which could suggest at first glance hydrogen evolution. Such an hypothesis has to be ruled out, because it would lead to a plateau for other electrode balance, which is actually not observed. Actually, for R = 0.5, the negative electrode (carbon) is highly overcapacitive leading to a flat profile for negative electrode voltage variation.

Using a reference electrode in a Swagelok cell makes it possible to extract the capacities for the positive and negative electrodes from the voltammograms of Fig. 3b. The discharge capacities obtained, presented in Fig. 4a, confirm the mechanisms previously discussed. Increasing the amount of cobalt oxide induces indeed an increase of the capacity that is linked to the AC electrode, and a decrease of the capacity of the cobalt oxide electrode. It should be
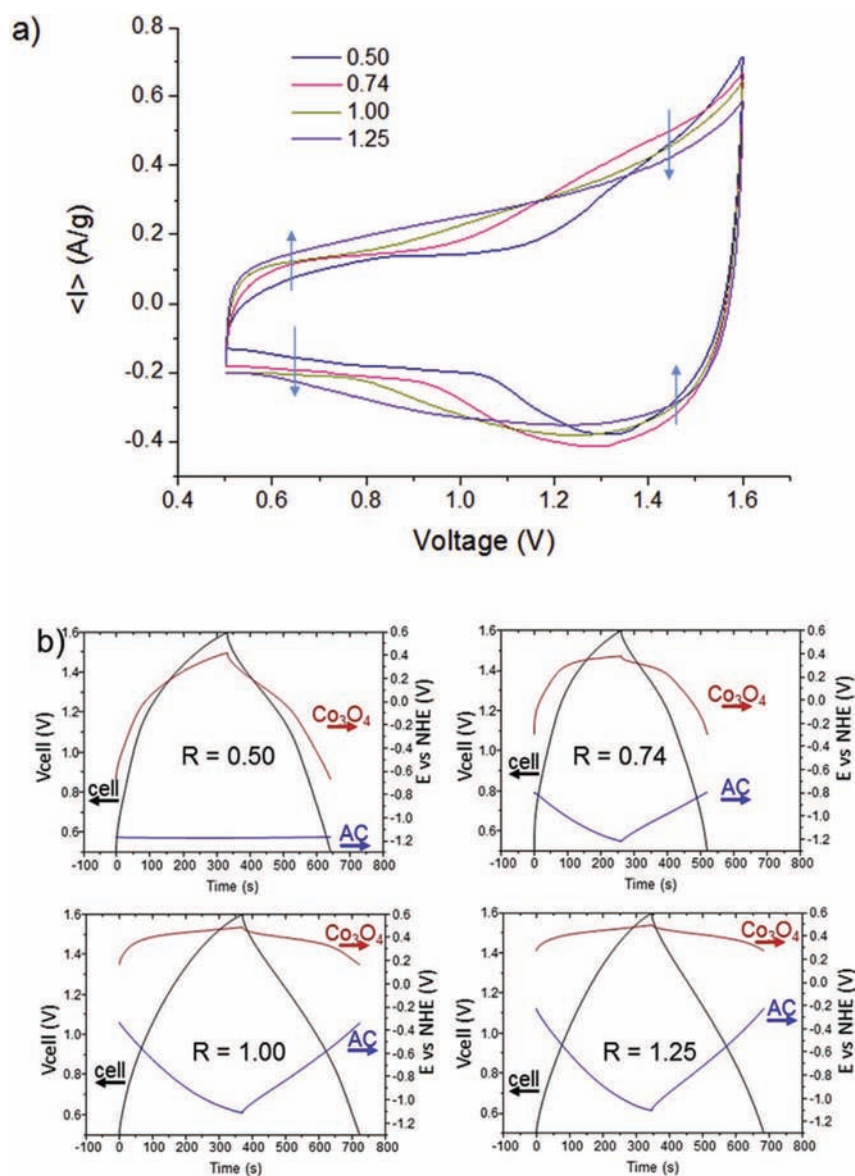
**Fig. 3.** Comparison of the voltammograms and charge/discharge curves, obtained for AC/nano-$Co_3O_4$ hybrid supercapacitors, exhibiting various weight ratio between the positive electrode and the negative one (R = 0.50, 0.74, 1.00 and 1.25). The measurements are performed in three-electrode Swagelock cell, in 5M-KOH, between 0.5 and 1.6 V, by (a) cyclic voltammetry and (b) galvanostatic cycling at 0.2 A $g^{-1}$.

noticed that the capacity values of both electrodes are equal (around 18 mAh $g^{-1}$) for the cell prepared with R = 0.74. This is in good agreement with the maximum capacities that were determined during the preliminary electrochemical study of the electrode materials (see section 3.2.1). In addition, on the basis of these maximum values, it is possible to calculate the operating percentage of the AC and cobalt oxide electrodes. As shown in Fig. 4b, the operating parts are quite weak (lower than 60%), whatever the values of R or the electrode nature. Even in the case of R = 0.50, for which only cobalt oxide is electrochemically active, only 56% of the maximum capacity of this material is extracted during the discharge. The only way to improve these operating percentages would consist in increasing the cell voltage, but it is not possible because, as shown in section 3.2.1, the oxidation of cobalt is in competition with hydrogen/oxygen release beyond 1.6 V.

The total discharge capacities are reported in Fig. 4c for the four cell configurations, together with the coulombic efficiencies, which were extracted from galvanostatic cycles of Fig. 3b. The capacities

determined for the various systems are located in a narrow domain, between 17 and 20 mAh $g^{-1}$. The supercapacitor prepared with R = 1.00 exhibits the highest discharge capacity (19.5 mAh $g^{-1}$ or 63.9 F $g^{-1}$ of total active material in the positive and negative electrodes), but the difference with the other systems is not really significant. The coulombic efficiencies are higher than 97% (except for R = 0.50), which suggests that a good stability in cycling should be reached.

### 3.2.3. Study at high rate

Energy and power densities are important parameters to characterize power sources such as supercapacitors. Ragone diagrams, which represent power densities vs energy densities, have therefore been established for the studied various cells. Average power and energy, denoted as $P_{mean}$ and $E_{mean}$ respectively, were determined on the basis of galvanostatic cycling, which was performed between 0.5 and 1.6 V, with currents ranging from 0.2 to 5 A $g^{-1}$. $P_{mean}$ is defined by the relation: $P_{mean} = \frac{\Delta V \cdot I}{m}$ (W kg − 1), with
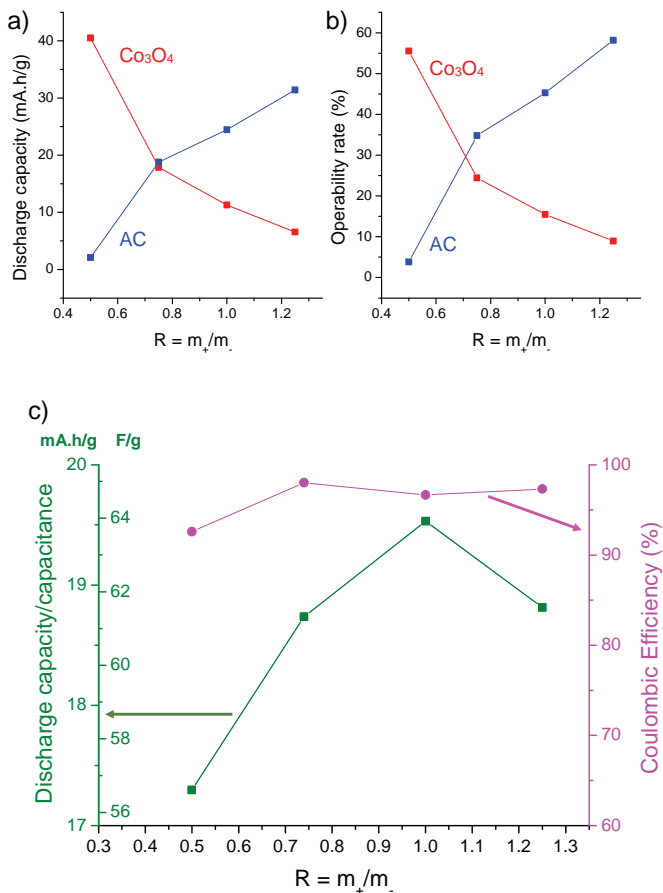
Fig. 4. Comparison of the electrochemical behaviors of AC/nano-Co$_3$O$_4$ hybrid super-capacitors exhibiting various weight ratio between the positive and negative electrode (R = 0.50, 0.74, 1.00 and 1.25). The data are extracted from cyclic voltammetry measurements in three-electrode Swagelock cells, in 5M-KOH, at 5 mV s$^{-1}$, between 0.5 and 1.6 V. (a) Discharge capacities and (b) operability rates associated to the positive and negative electrodes. The capacity values are relative to the active material weight in each electrode. (c) Discharge capacities and coulombic efficiencies of the complete cell. The capacities are relative to the total weight of active materials (cobalt oxide and activated carbon).

$\Delta V = (V_{max} + V_{min})/2$ ($V_{max}$ and $V_{min}$ are the voltage of finishing charge and discharge respectively), I is the applied current (A) and m the total mass of active material (kg). $E_{average}$ is deduced from $P_{mean}$, according to the relation: $E_{mean} = P_{mean} \cdot t$ (Wh kg$^{-1}$), where t corresponds to the discharge time. The results obtained for the 4 mass ratio (between positive and negative electrodes) are illustrated in Fig. 5. The data registered in the same conditions for a symmetric AC/AC cell are also reported for comparison purpose. From a general point of view, the energy densities of hybrid AC/nano-Co$_3$O$_4$ supercapacitors are higher than for the AC/AC cell. At low rate, the points characteristic of the four hybrid super-capacitors are close to each other, around 20 Wh kg$^{-1}$ for a power density of 209 W kg$^{-1}$. The energy densities are twice higher than those concerning the symmetric cell (10.2 Wh kg$^{-1}$). When power increases, the energy densities decrease, all the more rapidly as the R value, i.e. the relative mass of activated carbon, is weak. This behavior is due to the fact that the electrostatic charge storage in carbon is less affected by rate than the storage, essentially faradaic, in the cobalt oxide electrode.

Last but not least, the Ragone diagrams show that the highest energy is obtained for the AC/nano-Co$_3$O$_4$ supercapacitor with R = 1.25. Its energy density reaches 19.7 Wh kg$^{-1}$ at 212 W kg$^{-1}$, and 7.9 Wh kg$^{-1}$ for a power density of 5250 W kg$^{-1}$. This cell
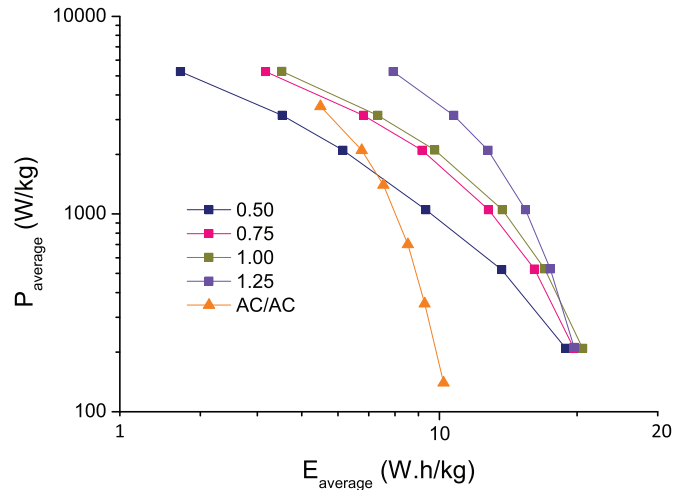


Fig. 5. Ragone diagrams of AC/nano-Co$_3$O$_4$ hybrid supercapacitors exhibiting various weight ratio between the positive and negative electrode (R = 0.50, 0.74, 1.00 and 1.25). The data obtained for a AC/AC symmetric supercapacitor in similar operating conditions between 0.5 and 1.6 V are displayed for comparison purpose.

configuration exhibits an evolution in power comparable to the symmetric AC/AC cell, but with energy densities twice higher. Within the range of tested ratios, the best performances are obtained for the highest ratio tested (R = 1.25). Going towards higher ratio would not be relevant because, as experimentally shown, the positive electrode is already partially charged and discharged for R = 1.25. Higher ratio would lower mean cell voltage as well as effective cell capacity. The fact that our hybrid capacitor showed higher power density than EDLC could appear as surprising at first sight, because cation intercalation reaction into Co$_3$O$_4$ is usually slower than charge/discharge of electric double layer. Nevertheless, in our hybrid devices, for R > 0.74, the Co$_3$O$_4$ electrode is over-capacitive, and therefore slightly stressed as compared to carbon electrode. As shown on discharge curves, the cell voltage is mainly driven by the carbon electrode, which is the one limiting the per-formances, instead of the intercalation kinetics of the positive electrode. In addition, the power density depends of course on the total mass of active materials. Then, the density of Co$_3$O$_4$ is lower than that of carbon one, which leads to higher power density.

### 3.3. Focus on the electrochemical behavior of the balanced hybrid supercapacitor (R = 0.74)

#### 3.3.1. Galvanostatic cycling

The cell has been submitted to galvanostatic cycling between 0.5 and 1.6 V, for current values ranging from 0.2 to 3 A g$^{-1}$. The charge/discharge curves obtained are gathered in Fig. 6; they exhibit three different domains. A potential jump takes place at the very begin-ning of charge and discharge, linked to the serial resistance of the cell, and increasing with the intensity values. Curved and hybrid portions are observed above 1.1 V, for charge and discharge, cor-responding to a redox process, i.e. oxidation of the cobalt electrode. The curve part that is located below 1.1 V is quasi linear and is characteristic of a capacitive behavior. As already mentioned in section 3.1, the electrochemical response of the supercapacitor is governed by AC for low cell voltage (lower than 1.1 V), and by cobalt oxide at higher voltage. In addition, when intensity increases, the discharge curve becomes more and more linear, and the capacities calculated from the discharge curves decrease from 18.7 mAh g$^{-1}$ at 0.2 A g$^{-1}$ down to 6.5 mAh g$^{-1}$ at 3 A g$^{-1}$. The behavior of the hybrid AC/nano-Co$_3$O$_4$ supercapacitor with R = 0.74 can therefore be
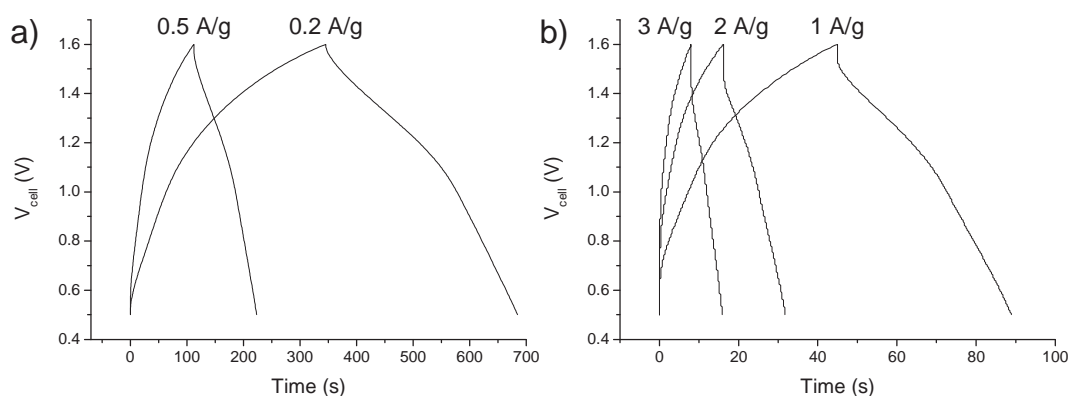
**Fig. 6.** Charge/discharge galvanostatic cycles of a AC/nano-Co₃O₄ charge balanced hybrid supercapacitor (weight ratio between the positive and negative electrodes R = 0.74). The measurements were performed with a three-electrode Swagelock cell in 5M-KOH, between 0.5 and 1.6 V, for the following currents: 0.2, 0.5 (a), 1, 2 and 3 (b) A g$^{-1}$.

considered as very close to that of a symmetric AC/AC cell at high rate, and tends towards that of battery, with higher capacities, at low rate.

### 3.3.2. Electrochemical ageing

The electrochemical ageing of the hybrid AC/nano-Co₃O₄ cell with R = 0.74 has been studied by cyclic voltammetry at 5 mV s$^{-1}$ in the 0.5–1.6 V range. The voltammograms collected over 3000 cycles are presented in Fig. 7a. After an activation during the first cycle, the shape of the subsequent cycles is quite similar. Fig. 7b shows the variation of discharge capacity and of coulombic efficiency vs cycle number. The electrochemical stability is quite good, since 82% of the initial capacity are retained after 3000 cycles. The ageing of the system is particularly discernible over the first 100 cycles, but the capacity loss is not more than 7% between cycle number 101 and cycle number 3000. As far as coulombic efficiency is concerned, the obtained values exceed 97%, which is higher than the lower limit corresponding to a correct reversibility of the system. Moreover, the coulombic efficiency increases slightly during the cycling (from 97.1 up to 98.9%), due to a weak repositioning of the potentials of the two electrodes.

### 3.4. Comparison with other aqueous systems

As previously detailed in the present paper, the configuration of the hybrid AC/nano-Co₃O₄ cell that leads to the best electrochemical performances corresponds to a mass ratio (R) between the positive and negative electrode of 1.25. This system exhibits indeed the best behavior at high power (weakest energy loss), even if the capacity (61.6 F g$^{-1}$) is not significantly different from the other compositions. In literature, the major part of the works refer to the AC/MnO₂ system, which exhibits capacitance values between 29 and 57.7 F g$^{-1}$ in neutral medium [12–20], and up to 63 F g$^{-1}$ for a graphene/MnO₂ composite electrode [21]. Among the numerous systems that have been tested in neutral medium, the AC/V₂O₅ system exhibits a capacitance of 32.5 F g$^{-1}$ and the AC/LiMn₂O₄ leads to attractive performances with more than 91 F g$^{-1}$ [22]. But the highest capacities are obtained in basic medium, for nickel or cobalt oxides/hydroxides, as shown by the hybrid cells based on mixed nickel-cobalt oxides (60–97 F g$^{-1}$) [23,24], cobalt hydroxides (72–77 F g$^{-1}$) [25–27] or nickel hydroxides (50.6–88.8 F g$^{-1}$) [28,29]. The highest capacity comes from a cell including aluminum substituted nickel hydroxide (127 F g$^{-1}$) [30]. Other systems in basic medium give less interesting results, such as the AC/MnO₂ system (44.4–62.4 F g$^{-1}$) [31,32] and AC/Fe₃O₄ (37.9 F g$^{-1}$) [33].

With values higher than 60 F g$^{-1}$, the capacities obtained for our AC/nano-Co₃O₄ hybrid supercapacitors put them in a good position among the complete hybrid cells in aqueous medium.
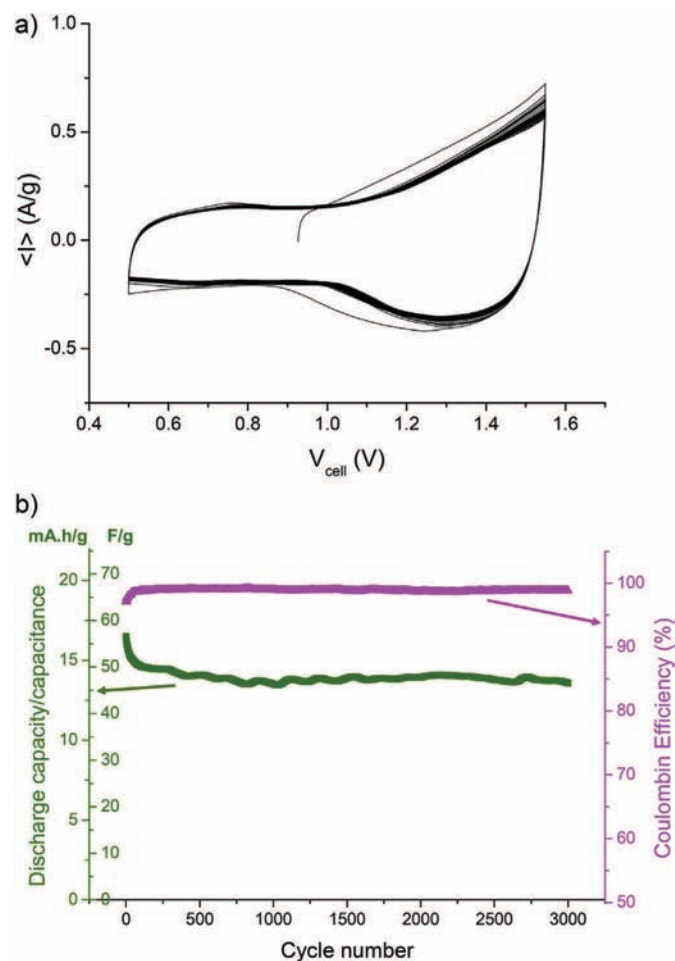


**Fig. 7.** (a) Cyclic voltammetry curves of AC/nano-Co₃O₄ charge balanced hybrid supercapacitor (weight ratio between the positive and negative electrodes R = 0.74). The measurements were performed with a three-electrode Swagelock cell in 5M-KOH, between 0.5 and 1.6 V, over 3000 cycles. (b) Variation of the discharge capacity and of the coulombic efficiency over 3000 cycles.

## 4. Conclusion

The behavior of AC/nano-$Co_3O_4$ supercapacitors has been studied in the 0.5–1.60 V optimal operating window. The investigation of various weight ratios between the positive (nano-$Co_3O_4$) and negative (AC) electrodes reveals an increasing contribution of the carbon electrode as its relative amount decreases. Except for the configuration with a ratio R (m+/m−) = 0.50, the studied systems exhibit similar features at low rate, with discharge capacities ranging from 17 to 20 mAh $g^{-1}$. Cycling at high rate allows to discriminate the various compositions and leads to the best performances for the cell with the highest amount of cobalt oxide (R = 1.25). In addition, the energy densities reached by this cell are twice higher than the values measured for a symmetric AC/AC cell in similar operating conditions. Such a behavior shows that the attempted energy density increase aimed in this work was reached. Nevertheless, in this optimal cell (R = 1.25), the operability rates of the cobalt oxide and AC are only 9 and 58% respectively, which suggests that the charges of both electrodes are only partially used, so that the stability upon cycling is improved with regard to a balanced cell. Last, the discharge capacity reached by the optimized AC/nano-$Co_3O_4$ supercapacitor (R = 1.25) (61.6 F $g^{-1}$) places this system among the best ones of its category.

## Acknowledgments

## Appendix A. Supplementary data

Supplementary data related to this article can be found at http://dx.doi.org/10.1016/j.jpowsour.2016.09.035.

## References

[1] K. Naoi, P. Simon, Interface 17 (2008) 34−37.
[2] G. Godillot, L. Guerlou-Demourgues, P.-L. Taberna, P. Simon, C. Delmas, Electrochem. Solid-State Lett. 14 (10) (2011) A139−A142.
[3] G. Godillot, P.-L. Taberna, B. Daffos, P. Simon, C. Delmas and L. Guerlou-Demourgues, Submitted to J. Electrochem. Soc.
[4] K.M. Shaju, L. Guerlou-Demourgues, G. Godillot, F. Weill, C. Delmas, J. Electrochem. Soc. 159 (12) (2012) A1934−A1940.
[5] G. Godillot, Hua Huo, M. Ménétrier, L. Bourgeois, L. Guerlou-Demourgues, C. Delmas, J. Phys. Chem. C 116 (2012) 26598−26607.
[6] G. Godillot, L. Guerlou-Demourgues, L. Croguennec, K.M. Shaju, C. Delmas, J. Phys. Chem. C 117 (2013) 9065−9075.
[7] P. Ratajczak, K. Jurewicz, F. Béguin, J. Appl. Electrochem. 44 (2013) 475−480.
[8] P. Ratajczak, K. Jurewicz, P. Skowron, Q. Abbas, F. Béguin, Electrochim. Acta 130 (2014) 344−350.
[9] M. He, K. Fic, E. Frackowiak, P. Novák, E.J. Berg, Energy Environ. Sci. 9 (2016) 623−633.
[10] E. Frackowiak, F. Béguin, Carbon 40 (2002) 1775−1787.
[11] K. Jurewicz, E. Frackowiak, F. Béguin, Appl. Phys. A 78 (2004) 981−987, http://dx.doi.org/10.1007/s00339-003-2418-8.
[12] L. Demarconnay, E. Raymundo-Pinero, F. Béguin, J. Power Sources 196 (2011) 580−586.
[13] M.S. Hong, S.H. Lee, S.W. Kim, Electrochem. Solid-State Lett. 5 (2002) A227−A230.
[14] T. Brousse, M. Toupin, D. Belanger, J. Electrochem. Soc. 151 (2004) A614−A622.
[15] V. Khomenko, E. Raymundo-Pinero, F. Béguin, J. Power Sources 153 (2006) 183−190.
[16] Y. Xue, Y. Chen, M.-L. Zhang, Y.-D. Yan, Mater. Lett. 62 (2008) 3884−3886.
[17] Q. Qu, Y. Shi, S. Tian, Y. Chen, Y. Wu, R. Holze, J. Power Sources 194 (2009) 1222−1225.
[18] C. Xu, H. Du, B. Li, F. Kang, Y. Zeng, J. Electrochem. Soc. 156 (2009) A435−A441.
[19] Q. Qu, L. Li, S. Tian, W. Guo, Y. Wu, R. Holze, J. Power Sources 195 (2010) 2789−2794.
[20] P.-C. Gao, A.-H. Lu, W.-C. Li, J. Power Sources 196 (2011) 4095−4101.
[21] Z. Fan, J. Yan, T. Wei, L. Zhi, G. Ning, T. Li, F. Wei, Adv. Funct. Mater. 21 (2011) 2366−2375.
[22] L.-M. Chen, Q.-Y. Lai, Y.-J. Hao, Y. Zhao, X.-Y. Ji, J. Alloys Compd. 467 (2009) 465−471.
[23] J.-W. Lang, L.-B. Kong, M. Liu, Y.-C. Luo, L. Kang, J. Electrochem. Soc. 157 (2010) A1341−A1346.
[24] C. Tang, Z. Tang, H. Gong, J. Electrochem. Soc. 159 (2012) A651−A656.
[25] Y.-G. Wang, L. Cheng, Y.-Y. Xia, J. Power Sources 153 (2006) 191−196.
[26] L.-B. Kong, M. Liu, J.-W. Lang, Y.-C. Luo, L. Kang, J. Electrochem. Soc. 156 (2009) A1000−A1004.
[27] L.-B. Kong, M. Liu, J.-W. Lang, Y.-C. Luo, L. Kang, J. Electrochem. Soc. 157 (2010) S9−S9.
[28] Y.-g. Wang, L. Yu, Y.-y. Xia, J. Electrochem. Soc. 153 (2006) A743−A748.
[29] Z. Tang, C.-h. Tang, H. Gong, Adv. Funct. Mater. 22 (2012) 1272−1278.
[30] J.-W. Lang, L.-B. Kong, M. Liu, Y.-C. Luo, L. Kang, J. Solid State Electrochem. 14 (2010) 1533−1539, http://dx.doi.org/10.1007/s10008-009-0984-1.
[31] A. Yuan, Q. Zhang, Electrochem. Commun. 8 (2006) 1173−1178.
[32] A. Yuan, X. Wang, Y. Wang, J. Hu, Energy Conver. Manage. 51 (2010) 2588−2594.
[33] X. Du, C. Wang, M. Chen, Y. Jiao, J. Wang, J. Phys. Chem. C 113 (2009) 2643−2646.